

Comparison of the Tissue Distribution and Metabolism of AN1284, a Potent Anti-Inflammatory Agent, After Subcutaneous and Oral Administration in Mice

Michal Weitman

Bar-Ilan University

Corina Bejar

Hebrew University School of Pharmacy

Michal Melamed

Hebrew University School of Pharmacy

Tehilla Weill

Hebrew University School of Pharmacy

Inessa Yanovsky

Bar-Ilan University

Shani Zeeli

Bar-Ilan University

Avraham Nudelman

Bar-Ilan University

Marta Weinstock (✉ martar@ekmd.huji.ac.il)

Hebrew University School of Pharmacy <https://orcid.org/0000-0002-4254-6779>

Research Article

Keywords: Amino-indoline derivative, Interleukin-6, liquid chromatography/mass spectrometry, metabolic oxidation, tissue distribution.

Posted Date: May 10th, 2021

DOI: <https://doi.org/10.21203/rs.3.rs-425679/v1>

License:   This work is licensed under a Creative Commons Attribution 4.0 International License.

[Read Full License](#)

Version of Record: A version of this preprint was published at Naunyn-Schmiedeberg's Archives of Pharmacology on July 26th, 2021. See the published version at <https://doi.org/10.1007/s00210-021-02125-y>.

Abstract

Purpose. To establish a liquid chromatography/mass spectrometry method to compare the tissue distribution and metabolism of AN1284 after subcutaneous and oral administration at doses causing maximal reductions in IL-6 in plasma and tissues of mice.

Methods. Lipopolysaccharide activated RAW 264.7 macrophages were used to detect the anti-inflammatory activity of AN1284 and its metabolites. Mice were given AN1284 by injection or gavage, 15 min before lipopolysaccharide. The reduction of IL-6 measured after 4h.

Results. AN1284 is metabolized to the indole (AN1422), a 7-OH derivative and its glucuronide. AN1422 had weaker anti-inflammatory activity than AN1284 in LPS-activated macrophages and in mice. Maximal reductions in IL-6 in plasma, brain and liver were seen after subcutaneous injection of (0.5 mg/kg). This dose was also most effective in reducing IL-6 in the liver after oral drug administration but 2.5 mg/kg was needed for the same reductions in plasma and brain. Peak concentrations after oral administration of AN1284 (2.5 mg/kg) were 5.5-fold higher in the liver but 7-, 11 and 19-fold lower in plasma, brain and kidneys than after injection of 0.5 mg/kg. Similar concentrations in the liver were achieved by AN1284 (1 mg/kg/day) administered in the drinking fluid, and 2.5 mg/kg/day, via subcutaneously-implanted mini-pumps. Although drug levels were only 12% of the peak seen after acute injection of 0.5 mg/kg, they significantly decreased hepatocellular damage, liver triglycerides and cholesterol in diabetic mice.

Conclusion. AN1284 can be given orally to treat chronic liver disease and its preferential concentration in the liver should limit potential adverse effects.

Introduction

An imbalance of pro- and anti-inflammatory cytokines occurs in many pathological conditions. These include among others, rheumatoid arthritis (Feldmann et al. 1996, Costa et al. 2018), ulcerative colitis (Strober and Fuss 2011), type 2 diabetes (Rehman and Akash 2016), acute liver failure (Granger and Remick 2005), acute lung disease (Dolinay et al. 2012) and non-alcoholic fatty liver disease (NAFLD) (Farrell et al. 2018). Most of the orally administered drugs used to treat these conditions do not provide adequate relief (Miossec 2014, Golabi et al. 2017, Damiao et al. 2019) and currently, no drug is effective for the treatment of NAFLD (Boeckmans et al. 2019). Although monoclonal antibodies or soluble receptors, given to block TNF- α are very effective in treating rheumatoid arthritis and ulcerative colitis, they have to be administered parenterally (Schwartzman and Morgan 2004) and are very expensive (Ollendorf et al. 2009). Moreover, they can increase the risk of tuberculosis and demyelination disorders (Khanna and Feagan 2015, Kemanetzoglou and Andreadou 2017) and cause autoimmune and severe allergic reactions due to autoantibodies (Jani et al. 2018). Since TNF- α and other cytokines are essential for immune regulation, inhibition of tumor growth, defense against pathogens and tissue regeneration, it

should be safer to reduce the pathogenic levels of cytokines than blocking their actions with monoclonal antibodies or soluble receptors to avoid these adverse effects.

For this purpose, we prepared a series of indoline derivatives that reduce the release of pro-inflammatory cytokines from lipopolysaccharide (LPS)-activated macrophages at picomolar concentrations (Zeeli et al. 2018). In mice with acute liver injury caused by LPS/D-galactosamine, subcutaneous (sc) injection of 3-(indolin-1-yl)-N-isopropylpropan-1-amine 2HCl (code named AN1284) (0.25–0.75 mg/kg) markedly reduced mortality, liver damage, the elevation of TNF- α and IL-6 in plasma and liver and alanine transferase (ALT) and aspartate aminotransferase in plasma. AN1284 also decreased DNA binding of Activator protein 1 to the level found in saline-injected controls (Finkin-Groner et al. 2017). Administration of AN1284 (2.5 and 5 mg/kg/24h) for two months via sc implanted Alzet mini-pumps to BSK-*db/db* mice with type 2 diabetes, significantly decreased renal damage, TNF- α , IL-18 and TGF- β levels and body fat. This treatment also improved kidney and liver function and preserved pancreatic β cell mass and insulin sensitivity (Permyakova et al. 2020). This method of administration was used to avoid the stress of daily injection and because AN1284 and other indoline derivatives were shown to be effective when injected subcutaneously in previous experiments (Finkin-Groner et al. 2015, Finkin-Groner et al. 2017, Shifrin et al. 2017).

As oral administration is more convenient than injections and has better patient compliance, the first aim of this study was to find the dose of AN1284 that would cause the maximum reduction in plasma and tissue cytokines in LPS-treated mice when given by gavage like that seen after sc injection. Previously it was shown that AN1284 is rapidly degraded by mouse and human microsomes (Maimon, 2016). Knowledge of the metabolism and pharmacokinetics of a drug intended for clinical use is essential for the prediction of the therapeutic outcome and any potential adverse effects. Thus, the second aim was to develop a liquid-chromatography mass spectral (LC-MS/MS) method sensitive enough to detect AN1284 and any metabolites in plasma and tissues and use it to compare drug distribution and metabolism after sc and oral administration. Lastly, we wanted to find the concentration of AN1284 that could be given chronically in the drinking fluid that would produce a similar amount of drug in the liver to that given by subcutaneously implanted mini-pumps, which was effective in reducing liver damage.

Materials And Methods

Animals

All experimental procedures in mice complied with the Principles of Laboratory Animal Care (NIH publication #85 – 23, revised 1985) and were performed according to protocols approved by the Ethics Committee of the Hebrew University. Male ICR mice, 7-8-weeks old, provided by Envigo (Jerusalem, Israel) were used for these experiments. The mice were housed in groups of 5 per cage in a pathogen-free unit under controlled 12 h light/12 h dark cycle (lights on at 7:00 and lights off at 19:00) and an ambient temperature of $21 \pm 1^\circ\text{C}$ and 40–50% humidity, with free access to standard rodent chow (Envigo, Israel) and water. The mice were acclimatized to the Animal facility for at least five days before the experiment.

Compounds and reagents

AN1284 (Molecular weight MW 291.26 gr/mol, free base 218.34 g/mol) and AN1422 (3-(indole-1-yl)-*N*-isopropylpropan-1-amine, (its oxidized metabolite, MW 216.33 g/mol) and the 4, 5 and 7-OH metabolites of AN1284 (MW 234.34 g/mol). LPS (from *Escherichia coli*, serotype (0111:B4), Verapamil and metoprolol were purchased from Sigma Aldrich and human and mouse liver microsomes, from Corning Inc. Rivastigmine hemitartrate was a gift from Novartis, Basle, Switzerland. LC-MS/MS grade methanol, ultra-high pressure liquid chromatography (UHPLC) grade water and acetonitrile (MeCN) were purchased from Biolab Ltd., Israel. GHP membranes were purchased from Pall Corporation, NY, USA. and formic acid from Merck (Darmstadt, Germany).

Measurement of nitric oxide and cytokines in LPS activated RAW 264.7 cells

The experiments were carried out as described in Zeeli et al., 2018, with minor modifications. RAW 264.7 cells (European Collection of Authenticated Cell Cultures (ECACC, passage 4–5) were seeded at a density of 50×10^3 cells per well in 96-well culture plates. AN1284 was added to the cells and medium containing 2% fetal calf serum to give final concentrations ranging from 1×10^{-13} – 1×10^{-7} M. Once the indole metabolite, (codenamed AN1422), and the 7-OH metabolite of AN1284, (codenamed AN1280), were identified, they were synthesized and added to RAW 264.7 cells at similar concentrations to those of AN1284. The cells were incubated for 2 h at 37°C prior to stimulation with (LPS, 2.5 µg/mL). After 8 h, supernatants were harvested for measurement of TNF-α and after 24 h for IL-6 and nitric oxide (NO) as previously described (Zeeli et al. 2018). At least three experiments using four or six replications of each concentration were performed.

Measurement of IL-6 in plasma and tissues

In previous studies, we showed that IL-6 protein could be reliably measured in plasma, brain and liver, 4 h after intraperitoneal (ip) injection of LPS (Finkin-Groner et al. 2015). We also found that the reduction of IL-6 by AN1284 in plasma was greater when the drug was given 15 min before LPS than after 30 min. Mice were injected subcutaneously with saline, 1 mL/100 g, or AN1284 (10–21 per dose) (0.05, 0.5 mg/kg or 2.5 mg/kg), dissolved in saline. Other mice were injected subcutaneously with AN1422, dissolved in DMSO, diluted 100-fold in saline, at doses of 0.44 or 2.2 mg/kg (8–15 mice per dose), or DMSO diluted 100-fold as vehicle control, 15 min before ip injection of LPS (5 mg/kg). Other groups of 7–16 mice were given water (10 mL/kg) or AN1284 (0.5, 2.5 or 10 mg/kg) by gavage, all 15 min before LPS. Four h later, the mice were deeply anesthetized with ketamine 100 mg/xylazine, 10 mg/kg and blood collected by cardiac puncture. The liver, brain and kidneys were rapidly removed, snap-frozen in liquid nitrogen and stored at -80 °C until assayed for IL-6 as previously described (Finkin-Groner et al. 2015).

Measurement of AN1284 and AN1422 in plasma and tissues

Oral administration of AN1284 (2.5 mg/kg, 2.2 mg/kg base) produced a maximal reduction in IL-6 in plasma of LPS injected mice, similar to that seen after 0.5 mg/kg (0.44 mg/kg base) injected sc. Therefore, these doses were used to measure the concentrations of AN1284 and its metabolites in plasma and tissues and four mice were given saline to serve as controls. After drug administration by the oral or sc route, the mice were deeply anesthetized with ketamine (100 mg/kg) + xylazine (10 mg/kg) and decapitated 5, 10, 20, 30, 45 or 60 min later. Blood was collected into tubes containing 10 μ L EDTA (0.5M), liver, brain and kidneys were rapidly removed, snap-frozen in liquid nitrogen and stored at -80 °C.

Since chronic sc administration of AN1284 by mini-pumps at concentrations of 1 and 2.5 mg/kg/24 h significantly reduced signs of liver damage in mice on a high fat diet (unpublished observations) or in *dbdb* mice with type 2 diabetes (Permyakova et al. 2020), we also gave these doses and method of administration to two groups of 8 mice and measured the concentration of AN1284 and the indole metabolite in the liver. After we found that oral and sc administration of AN1284 (0.5 mg/kg) caused a similar reduction in liver cytokines, we gave the drug in the drinking water to groups of 8 mice to provide concentrations of 0.25, 0.5 or 1 mg/kg/day and measured the levels of drug in the liver.

The urinary excretion of AN1284 and any metabolites was measured in seven mice, injected sc with AN1284 (0.5 mg/kg) or given (2.5 mg/kg) by gavage that were housed in individual metabolism cages. Urine was collected for 24 h, passed through 0.45 μ m filters. The pH was measured and the samples stored at -80 °C until analyzed by LC-S/MS.

Samples collected from all mice given AN1284 or saline were prepared for LC-MS/MS analysis as follows. To 160 μ L of plasma, were added 20 μ L of internal standard solution, (rivastigmine 750 ng/mL) and 20 μ L of ultra-pure water. The mixture was vortexed for five min and then allowed to stand for a further five min and the procedure repeated three times. To precipitate proteins, 300 μ L of ice-cold HPLC grade MeOH were added to each sample which was vortexed for 10 min and allowed to stand for another 10 min and also repeated three times. The samples were centrifuged at 20,800 g at 4°C for 15 min, the supernatants were withdrawn to an Eppendorf tube and 200 μ L were filtered through 0.25 μ M GHP membranes and stored at -80 °C until injection into the LC-MS/MS instrument. Samples from the brain and liver were prepared as described for plasma with minor modifications. The tissues were homogenized (100 mg/mL, Polytron, Kinematia GmbH, Germany) in phosphate buffered saline. Twenty μ L of internal standard were added to 180 μ L of tissue homogenate, followed by MeOH and treated as described for plasma. Calibration curves for different concentrations of AN1284 and AN1422 added to plasma, brain, kidney or liver homogenates prepared from control mice were also run for each experiment. The equation ($y = a + bx$) for each curve was obtained by linear least-squares regression of the measured peak area (y) versus the concentration added to the biological matrix (x), corrected for the peak area of the internal standard rivastigmine, added to each sample (Fig. 1D). After measurement of the volume and pH, 200 μ L of urine samples were stored in vials at -80 °C until injection into the LC-MS/MS instrument.

Analysis of plasma, tissue and urine samples

LC-MS/MS provides a powerful tool for the detection and quantification of specific analytes in mixtures from biological extracts that contain a number of compounds. Since many compounds may share the same exact mass, a combination of the following parameters distinguishes the desired component from analogs in the extract: 1. Retention time of the compound on the column; 2. Exact mass of the molecule, (i.e. precursor ion); 3. Unique ionic fragments of the molecule obtained in a collision cell that are specific because of its structure and functional groups. By manipulating the extracted ion chromatogram (EIC) obtained, which ignores irrelevant ions and focusing only on a specific ion fragment, one can draw the chromatogram of the desired specific compound. Therefore, even though several compounds are eluted simultaneously, information on each can be obtained separately (as shown in Fig. 1a).

All the equipment for the analyses was from Agilent technologies and consisted of a 6545 QTOF mass spectrometer was equipped with an electrospray ionization interface (ESI) coupled to a 1260 UHPLC, a G4204A quaternary pump, G4226A ALS auto-sampler, and G1316C thermostatted column compartment. UHPLC was carried out on a ZORBAX RRHD Eclipse Plus C18, 95Å, 2.1 x 50 mm, 1.8 µm column, or on a Poroshell 120 EC-C18, 4.6 x 50 mm, 2.7 µm column with water (0.1% formic acid)-MeCN gradient elution, from 5 to 95% MeCN for 10 min at a flow rate of 0.5 mL/min. Twenty µL of each sample and standards were injected into the LC-MS/MS instrument in triplicate and an average peak area of three analyses was calculated. The methanol solution was injected as a blank within a sequence of samples to confirm that there was no cumulative carryover. Mass spectral parameters were optimized for each compound by varying the fragmentor voltage of the ion source for scan mode and collision energy for product ion mode (MS/MS). Specific parameters of the ion source were readjusted. The ESI was operated in positive mode. The source temperature was set to 350°C and ion spray voltage was 4.5 kV. Standards were prepared of 1 mg/mL in methanol. Urine samples were injected into the LC-MS/MS machine without further preparation.

Identification of additional metabolites of AN1284

To identify the additional OH-metabolite of AN1284 detected in the urine after oral administration, the 4- and 5-OH analogs of AN1284 were synthesized as dihydrochloride salts using a similar procedure as that described for the *p*-toluene sulfonic acid salt of the 7-OH derivative of AN-1284 reported by Zeeli et al., (2018). A direct MS/MS analysis (no HPLC separation) for the three substances revealed that the position of the OH group did not affect the MS/MS fragmentation and the spectra of all three compounds were identical. However, we found that the position of the OH group dramatically influenced the retention time of the compounds on a LC column. Therefore, we injected urine from control mice to which was added amounts of the individual compounds into the LC-MS/MS apparatus as described for the analysis of the metabolites found in urine after administration of AN1284 to the mice. We found that only the 7-OH substituted derivative, (AN1280) had the same retention time as the metabolite found in the urine of drug treated mice, confirming the position of metabolic oxidation.

Statistical analysis

All doses and concentrations of AN1284 and AN1280 are expressed in terms of its 2HCl salt and AN1422 as a free base, and the results are presented as the mean \pm STD or SEM for measurements in macrophages. Differences in the levels of NO, TNF- α and IL-6 between similar concentrations of AN1284 and AN1422 released from RAW 264.7 cells and % of levels of IL-6 after saline and LPS induced by different doses of AN1284 were analyzed by ANOVA using IBM SPSS Statistics Version 19 followed by Duncan's *post hoc* test. A *p* value of < 0.05 was considered to be significant.

Results

Metabolism of AN1284

In samples prepared from mice given AN1284, a small increase in the level of the total ion chromatogram, that contains the information of all the ions found in the sample) was observed at a retention time close to that of AN1284 (Fig. 1a). The MH^+ ion of AN1284 is 219.185 and the MS spectrum of that zone in the chromatogram revealed an increase of the mass of 217.169 that displayed Gaussian behavior. This was not observed in solutions of AN1284 unexposed to biological media. Calculations of the difference between parent ions for the drug AN1284, 219.185 [MH^+] and its metabolite 217.169 [MH^+] corresponded to the indole with an exact mass of two fewer hydrogens. To confirm the identity of this metabolite, we compared the mass spectral parameters, retention time, ion parent mass and daughter ion peaks of AN1284 to that of the indole AN1422 (Zeeli et al. 2018). AN1284 and AN1422 share a common product ion of 132.080, indicating that the loss of the 2 hydrogens also occurs under the conditions of the collision cell-electric voltage and nitrogen bombardment. Although AN1284 contains two amine moieties and AN1422, only one, a comparison of their ion efficiencies revealed that AN1422 ionizes five times better than AN1284. Therefore, although the levels of AN1284 in the plasma and tissues are higher than those of AN1422, the area under the curve of the peak of AN1284 is lower.

Reduction of NO and cytokines by AN1284, and AN1422 in LPS activated RAW 264.7 macrophages

The increase in NO and cytokines in response to LPS in macrophages in the various experiments ranged from 1.0-3.7 μ M for NO, from 1.0-4.5 nM for TNF- α and from 2.8-17.8 nM for IL-6. AN1284 (0.1 μ M) significantly reduced NO, TNF- α and IL-6, $p < 0.01$. Peak reductions were seen at a concentration of 100 μ M. AN1422 was less effective than AN1284 in reducing NO and both cytokines and the peak reduction at 100 μ M was similar to that of 0.1 μ M of AN1284. AN1280 was less effective than AN1284 in reducing NO and TNF- α but not IL-6 (Fig. 2).

Reduction by AN1284 and AN1422 of IL-6 in plasma and tissues of LPS injected mice

In control mice given saline, the concentrations of IL-6 in plasma, brain and liver, 4 h after ip injection of LPS were 7.41 ± 0.12 ng/mL, 0.50 ± 0.04 ng/gm and 0.60 ± 0.04 ng/gm, respectively. AN1284 (0.5 mg/kg) injected 15 min before LPS caused maximal reductions in IL-6 in plasma, brain and liver of 31, 38 and 36%, respectively. Subcutaneous injection of AN1422 (0.44 and 2.2 mg/kg) reduced IL-6 significantly only in plasma (Table 1). When given orally, AN1284 (0.5mg/kg) reduced IL-6 in the liver by 34.6%, but only by 15 and 20% in plasma and brain, in which 2.5 mg/kg was needed to cause similar reductions in IL-6 to those seen after sc injection of 0.5 mg/kg.

Previously, we had shown that a sc injection of AN1284 could lower TNF- α in plasma of LPS injected mice (Zeeli et al. 2018). Because of the important role played by TNF- α in inflammatory disease, we measured the cytokine in plasma samples collected after oral administration of AN1284. At a dose of 2.5 mg/kg, AN1284 lowered plasma levels of TNF- α by $41.4 \pm 18.4\%$.

Concentrations of AN1284 and AN1422 in plasma and tissues

To compare plasma and tissue distribution of AN1284 and any metabolites after sc and oral administration, we used doses of 0.5 mg/kg and 2.5 mg/kg, respectively because they caused similar maximal reductions in IL-6 in plasma and tissues. The lowest detectable amount of AN1284 was 1.25 ng/mL and of AN1422, 0.125 ng/mL. The concentrations time curves of AN1284 and its metabolite in plasma and tissues after administration of these doses of AN1284 are shown in Figs. 3 a & b. Within five min of sc injection, peak levels of AN1284 were seen in plasma and kidneys and after ten min, in the brain and liver.

AN1284 was also rapidly absorbed after oral administration, but the relative distribution in plasma and tissues and the amounts of drug and metabolite differed substantially from those after sc injection. Thus, drug levels peaked at 5 min in the liver and only after 10 min, in plasma, brain and kidneys. The time course of the indole metabolite, AN1422 followed those of AN1284 (Figs 3a and b) and are and are shown in Table 3, expressed as % of those of the parent drug in plasma and tissues. After sc injection of AN1284 (0.5 mg/kg) levels of AN1422 ranged from 32-40% of those of the parent drug in plasma and tissues. When AN1284 (2.5 mg/kg) was given orally, the proportion of metabolite remained unchanged in the liver from that after injection but, in plasma, kidneys and brain it reached 57, 63% and 90%, respectively (Table 2).

The concentrations of AN1284 and AN1422 in the liver of mice given two doses of the drug chronically via sc implanted mini-pumps or three doses in the drinking fluid are shown in Table 3. Similar concentrations were achieved with 2.5 mg/kg/day via sc mini-pumps and 1 mg/kg/day in the drinking fluid. However, as might be expected, there was more inter-mouse variability when given by the latter route. The peak concentrations of the metabolite expressed as a % of those of the parent drug were similar when the drug was given by acute administration or chronically by each route (Table 3).

Cumulative 24h excretion of AN1284 and metabolites in urine

Despite the relatively high concentrations of AN1284 in the kidneys after sc injection, the 24 h urinary levels were only 0.38% of the administered dose (Table 4). They were even smaller, about 0.007%, after oral administration of a 5-fold higher dose, in keeping with the much lower concentrations of AN1284 found in the kidneys when given by this route. The low excretion could be explained by the urinary pH of 7.0-7.5 that would favor reabsorption of the basic drug. To discover any hydrophilic metabolites of AN1284 that would be more readily excreted, we scanned the urine samples and found two more drug-related species, an OH derivative and its glucuronide. The OH derivative was identified by an analysis of its daughter ion peaks: 324.108, 235.180, 148.076 and 100.112, which is shared by AN1284 (Fig. 1b). The concentrations of AN1280 in 24 h urine collections were about 1.4% of the dose administered orally. Since the 7-OH glucuronide was not available for the preparation of calibration curves, we were unable to measure the actual amounts in the urine. However, by comparing the peak areas of the glucuronide to those of AN1280, we estimated that there was probably twice as much after sc injection of AN1284, and almost 15 times as much of the glucuronide after oral administration (Table 4).

The smallest amount of AN1280 that was detectable in solution was 4.6 ng/ml (equivalent to a tissue concentration of 52 ng/gm). Five and ten minutes after oral administration of AN1284, the concentrations of AN1280 in the livers of three of the seven mice in which we were able to measure it were 692 ± 45 ng/gm and 410 ± 17 ng/gm, respectively, but were below the limits of detection in plasma and kidneys. By contrast, it was possible to measure the 7-OH glucuronide in the liver, plasma and kidneys in all the mice at both time points. Estimation of the amounts of the glucuronide from a comparison of the peak areas relative to those of the 7-OH derivative showed them to be about 50 times higher in the liver, five and ten min after drug administration. The estimated concentrations of the glucuronide in plasma and kidneys, like those of AN1284, were higher at ten than at five min.

Discussion

In all our previous studies, the indoline-based compounds that showed a beneficial effect in models of acute or chronic inflammatory conditions were given by sc injection (Finkin-Groner et al. 2015, Shifrin et al. 2016, Finkin-Groner et al. 2017, Shifrin et al. 2017). This route was also used for chronic administration of AN1284 via subcutaneously implanted mini-pumps in mice with diabetic mice with kidney and liver damage, to avoid the stress of daily injection (Permyakova et al. 2020). We now show that after its elevation by LPS, a sc injection of 0.5 mg/kg produced a maximal reduction of 31–38% in IL-6 in plasma, brain and liver and TNF- α , in plasma. This dose also reduced in IL-6 in the liver by 35% when given by gavage. To decrease this cytokine in brain and plasma by similar amounts it was necessary to give 2.5 mg/kg.

AN1284 is rapidly metabolized by preparations of mouse and human liver microsomes. Thus, using LC-MS/MS analysis, we identified the indole, AN1422 as a major metabolite in blood and tissues of mice.

This confirms a similar indoline to indole oxidative metabolism reported by Sun et al., (Sun et al. 2007), who showed that several different cytochrome P450 enzymes, including are CYP2C19 and CYP3A4, can convert indolines to indoles. AN1422 has anti-inflammatory activity in cells but at none of the concentrations tested did it reach the efficacy of AN1284. This accords with our previous finding that indole derivatives are less potent as anti-inflammatory agents than indolines (Yanovsky et al. 2012, Furman et al. 2014).

As might be expected with a lipophilic compound (Lin and Lu 1997), AN1284 was rapidly absorbed after sc administration and reached 6 and 21-fold higher concentrations in the brain and kidneys than in plasma and liver. This explains why a dose of 0.05 mg/kg caused a significant reduction of IL-6 of 22.3% in the brain but not in plasma or liver. The amounts of the indole metabolite relative to those of the parent drug were similar in plasma and tissues.

By contrast, oral administration of AN1284 resulted in 47 fold higher concentrations in the liver than in plasma, and only 2 and 6 fold higher concentrations in the brain and kidneys. This accords with the finding of a maximal reduction of IL-6 in the liver at 0.5 mg/kg, the lowest dose tested. The relative levels of the metabolite in plasma, brain and kidneys were almost double those after sc injection, probably because more than 5 fold higher amounts were formed in the liver within 5 min and the lipophilicity of AN1422 would ease its entry into the brain and kidneys.

The lower plasma concentration of AN1284 when given by gavage at a dose of 2.5 mg/kg than after 0.5 mg/kg by sc injection indicates that much of the drug was removed before reaching the circulation. This can be explained by the passage of the entire blood supply of the upper gastrointestinal tract (GIT) through the liver before reaching the systemic circulation (Leahy et al. 2000). The GIT and liver contain large amounts of the enzyme, CYP3A which is known to play a role in the first-pass metabolism of many orally dosed drugs (Kato 2008).

Indapamide, is another indoline, that is oxidized by liver microsomal enzymes to the indole and a 5-OH derivative (Sun et al. 2009). In the rat, indapamide is converted to the 2- and 3- and 5-OH metabolites, together with their glucuronides (Klunk et al. 1983). In the current study in mice, we found that AN1284 is oxidized to a 7-OH metabolite and its glucuronide. (Fig. 4). If other metabolites were formed, they were below the limits of detection. No evidence was found for oxidation in any other part of the molecule, or of the indole, AN1422.

Glucuronidation is an enzyme reaction process catalyzed by UDP-glucuronosyl transferases and is often a secondary step after metabolites are produced by phase I reactions such as hydrolysis, hydroxylation and dealkylation (Yang et al. 2017). As shown for many other compounds, glucuronides are formed in the GIT and liver, and stored in the gallbladder from which they can be released from the bile to the gut, excreted in the feces or undergo recycling to the parent drug (Roberts et al. 2002). Relatively high levels of the 7-OH metabolite and its glucuronide were already formed in the liver, five min after oral administration of AN1284 and explains the presence of larger amounts of this metabolite in the urine. After sc injection

of AN1284 (0.5 mg/kg), the 7-OH derivative and its glucuronide were below the level of detection in the liver but were measurable in the 24 h urine samples.

We had previously shown that chronic administration of AN1284, in diabetic mice at a dose of 2.5 mg/kg/day by mini-pumps resulted in a concentration in the kidneys of 140 ng/g (Permyakova et al. 2020). This was sufficient to reduce significantly the elevated protein expression of inflammatory markers MCP1, TNF α , TGF β and IL-18 and prevent the severe enlargement of the glomerulus and of Bowman's capsule. As expected, the concentrations in the liver produced by this method of drug administration were much lower (26.4 ng/g) than in the kidneys, but sufficient to decrease hepatocellular damage, liver triglyceride and cholesterol contents (Permyakova et al. 2020). These concentrations were only 9.3% and 12.7% of the peak levels seen after a single dose in liver and kidney, respectively. In preliminary experiments in mice with existing fatty liver disease, we found that AN1284 (1 mg/kg/day) given by this route was sufficient to reduce hepatosis and fibrosis. When we administered the drug in the drinking fluid at concentrations of 0.5 and 1 mg/kg/day, we obtained similar hepatic levels to those achieved by subcutaneously implanted mini-pumps. This suggests that this method of chronic oral administration mice, or by a sustained release formulation in humans, could be successful for the treatment of liver damage induced by a high-fat diet.

The activity of CYP3A, which may be responsible for oxidizing AN1284 to the indole, has been reported to be impaired in NAFLD (Cobbina and Akhlaghi 2017). However, this metabolic change should not lessen the beneficial effect of AN1284 in NAFLD or diabetes if it reduces the metabolites of AN1284 produced by this enzyme. Moreover, unlike other drugs that undergo first-pass metabolism in the liver, it is not necessary to increase the dose to obtain therapeutic concentrations for treating chronic liver disease. The higher amounts of the drug in the liver than in other tissues should reduce any of its potential adverse effects when used to treat chronic liver disease. It remains to be determined whether oral administration of AN1284 can also reverse liver damage in human subjects with this condition.

Conclusions

AN1284 is a novel, indoline derivative with anti-inflammatory activity at picomolar concentrations. It can prevent tissue damage in a mouse model of chronic liver and kidney disease when given by sc implanted mini-pumps. AN1284 also shows anti-inflammatory activity in the liver after oral administration at a dose similar to that after sc injection but at a five times higher dose is required to reduce IL-6 in the brain and plasma. The several-fold higher concentrations of unchanged drug found in the liver than in plasma and other organs make it an ideal drug for treating liver disease. Because of the short half-life of the drug, both in plasma and the liver, it may be preferable to administer it as an oral, sustained-release formulation.

Declarations

Ethical Approval

All experimental procedures in mice complied with the Principles of Laboratory Animal Care (NIH publication #85-23, revised 1985) and were performed according to protocols approved by the Ethics Committee of the Hebrew University.

Consent to Participate

Not applicable

Consent to Publish

Not applicable

Authors Contributions

All authors read and approved the manuscript and all data were generated in-house and no paper mill was used.

MiW performed all analytical and mass spectral studies.

CB, and MM, performed all the experiments in mice.

TW performed the experiments in RAW cells.

IY and SZ performed all the chemical syntheses.

AN Supervised the spectral analyses and chemical syntheses.

MaW conceived and designed the research analyzed the data and wrote the paper.

Acknowledgments

We thank Donna Schorer-Apelbaum for performing the graphics and statistical analyses and Yulia Shenberger and Bruria Schmerling for help with the LC-MS/MS analysis.

Funding

This research did not receive any specific grant from funding agencies in the public, commercial, or not-for-profit sectors.

Competing Interests

The authors declare no competing interest.

Availability of data and materials

Available

References

1. Boeckmans J, Natale A, Rombaut M, Buyl K, Rogiers V, De Kock J, Vanhaecke T, R MR (2019) Anti-NASH Drug Development Hitches a Lift on PPAR Agonism. *Cells* 9(1):37
2. Cobbina E, Akhlaghi F (2017) Non-alcoholic fatty liver disease (NAFLD) - pathogenesis, classification, and effect on drug metabolizing enzymes and transporters. *Drug Metab Rev* 49:197–211
3. Costa NT, Iriyoda TMV, Alfieri DF, Simao ANC, Dichi I (2018) Influence of disease-modifying antirheumatic drugs on oxidative and nitrosative stress in patients with rheumatoid arthritis. *Inflammopharmacology* 26:1151–1164
4. Damiao A, de Azevedo MFC, Carlos AS, Wada MY, Silva TVM, Feitosa FC (2019) Conventional therapy for moderate to severe inflammatory bowel disease: A systematic literature review. *World J Gastroenterol* 25:1142–1157
5. Dolinay T, Kim YS, Howrylak J, Hunninghake GM, An CH, Fredenburgh L, Massaro AF, Rogers A, Gazourian L, Nakahira K, Haspel JA, Landazury R, Eppanapally S, Christie JD, Meyer NJ, Ware LB, Christiani DC, Ryter SW, Baron RM, Choi AM (2012) Inflammasome-regulated cytokines are critical mediators of acute lung injury. *Am J Respir Crit Care Med* 185:1225–1234
6. Farrell GC, Haczeyni F, Chitturi S (2018) Pathogenesis of NASH: How Metabolic Complications of Overnutrition Favour Lipotoxicity and Pro-Inflammatory Fatty Liver Disease. *Adv Exp Med Biol* 1061:19–44
7. Feldmann M, Brennan FM, Maini RN (1996) Role of cytokines in rheumatoid arthritis. *Annu Rev Immunol* 14:397–440
8. Finkin-Groner E, Finkin S, Zeeli S, Weinstock M (2017) Indoline derivatives mitigate liver damage in a mouse model of acute liver injury. *Pharmacol Rep* 69:894–902
9. Finkin-Groner E, Moradov D, Shifrin H, Bejar C, Nudelman A, Weinstock M (2015) Indoline-3-propionate and 3-aminopropyl carbamates reduce lung injury and pro-inflammatory cytokines induced in mice by LPS. *Br J Pharmacol* 172:1101–1113
10. Furman S, Nissim-Bardugo E, Zeeli S, Weitman M, Nudelman A, Finkin-Groner E, Moradov D, Shifrin H, Schorer-Apelbaum D, Weinstock M (2014) Synthesis and in vitro evaluation of anti-inflammatory activity of ester and amine derivatives of indoline in RAW 264.7 and peritoneal macrophages. *Bioorg Med Chem Lett* 24:2283–2287
11. Golabi P, Bush H, Younossi ZM (2017) Treatment Strategies for Nonalcoholic Fatty Liver Disease and Nonalcoholic Steatohepatitis. *Clin Liver Dis* 21:739–753
12. Granger J, Remick D (2005) Acute pancreatitis: models, markers, and mediators. *Shock* 24(Suppl 1):45–51
13. Jani M, Dixon WG, Chinoy H (2018) Drug safety and immunogenicity of tumour necrosis factor inhibitors: the story so far. *Rheumatology* 57:1896–1907
14. Kato M (2008) Intestinal first-pass metabolism of CYP3A4 substrates. *Drug Metab Pharmacokinet* 23:87–94

15. Kemanetzoglou E, Andreadou E (2017) CNS Demyelination with TNF-alpha Blockers. *Curr Neurol Neurosci Rep* 17:36
16. Khanna R, Feagan B (2015) Safety of infliximab for the treatment of inflammatory bowel disease: current understanding of the potential for serious adverse events. *Expert Opin Drug Saf* 14:987–997
17. Klunk LJ, Ringel S, Neiss ES (1983) The disposition of ¹⁴C-indapamide in man. *J Clin Pharmacol* 23:377–384
18. Leahy DJ, Dann CE 3rd, Longo P, Perman B, Ramyar KX (2000) A mammalian expression vector for expression and purification of secreted proteins for structural studies. *Protein Expr Purif* 20:500–506
19. Lin JH, Lu AY (1997) Role of pharmacokinetics and metabolism in drug discovery and development. *Pharmacol Rev* 49:403–449
20. Maimon I (2016) Stability and Pharmacokinetics Assessments of AN1284 and AN1297 LS049 Study Report
21. Miossec P (2014) Introduction: 'Why is there persistent disease despite aggressive therapy of rheumatoid arthritis?'. *Arthritis Res Ther* 16:113
22. Ollendorf DA, Klingman D, Hazard E, Ray S (2009) Differences in annual medication costs and rates of dosage increase between tumor necrosis factor-antagonist therapies for rheumatoid arthritis in a managed care population. *Clin Ther* 31:825–835
23. Permyakova A, Gammal A, Hinden L, Weitman M, Weinstock M, Tam J (2020) A Novel Indoline Derivative Ameliorates Diabetes-Induced Chronic Kidney Disease by Reducing Metabolic Abnormalities. *Front Endocrinol (Lausanne)* 11:91
24. Rehman K, Akash MS (2016) Mechanisms of inflammatory responses and development of insulin resistance: how are they interlinked? *J Biomed Sci* 23:87
25. Roberts MS, Magnusson BM, Burczynski FJ, Weiss M (2002) Enterohepatic circulation: physiological, pharmacokinetic and clinical implications. *Clin Pharmacokinet* 41:751–790
26. Schwartzman S, Morgan GJ Jr (2004) Does route of administration affect the outcome of TNF antagonist therapy? *Arthritis Res Ther* 6(Suppl 2):S19–S23
27. Shifrin H, Moradov D, Bejar C, Schorer-Apelbaum D, Weinstock M (2016) Novel indoline derivatives prevent inflammation and ulceration in dinitro-benzene sulfonic acid-induced colitis in rats. *Pharmacol Rep* 68:1312–1318
28. Shifrin H, Mouhadeb O, Gluck N, Varol C, Weinstock M (2017) Cholinergic Anti-Inflammatory Pathway Does Not Contribute to Prevention of Ulcerative Colitis by Novel Indoline Carbamates. *J Neuroimmune Pharmacol* 12:484–491
29. Strober W, Fuss IJ (2011) Proinflammatory cytokines in the pathogenesis of inflammatory bowel diseases. *Gastroenterology* 140:1756–1767
30. Sun H, Ehlhardt WJ, Kulanthaivel P, Lanza DL, Reilly CA, Yost GS (2007) Dehydrogenation of indoline by cytochrome P450 enzymes: a novel "aromatase" process. *J Pharmacol Exp Ther* 322:843–851

31. Sun H, Moore C, Dansette PM, Kumar S, Halpert JR, Yost GS (2009) Dehydrogenation of the indoline-containing drug 4-chloro-N-(2-methyl-1-indolinyl)-3-sulfamoylbenzamide (indapamide) by CYP3A4: correlation with in silico predictions. *Drug Metab Dispos* 37:672–684
32. Yang G, Ge S, Singh R, Basu S, Shatzer K, Zen M, Liu J, Tu Y, Zhang C, Wei J, Shi J, Zhu L, Liu Z, Wang Y, Gao S, Hu M (2017) Glucuronidation: driving factors and their impact on glucuronide disposition. *Drug Metab Rev* 49:105–138
33. Yanovsky I, Finkin-Groner E, Zaikin A, Lerman L, Shalom H, Zeeli S, Weill T, Ginsburg I, Nudelman A, Weinstock M (2012) Carbamate derivatives of indolines as cholinesterase inhibitors and antioxidants for the treatment of Alzheimer's disease. *J Med Chem* 55:10700–10715
34. Zeeli S, Weill T, Finkin-Groner E, Bejar C, Melamed M, Furman S, Zhenin M, Nudelman A, Weinstock M (2018) Synthesis and Biological Evaluation of Derivatives of Indoline as Highly Potent Antioxidant and Anti-inflammatory Agents. *J Med Chem* 61:4004–4019

Tables

Table 1. Percent reduction by AN1284 and AN1422 of LPS-induced elevation of IL-6 in plasma and tissues

| | Dose (mg/kg) | Plasma | Brain | Liver |
|--------------------------------------|--------------|--------------------------------|--------------------------------|--------------------------------|
| <i>Subcutaneous injection</i> | | | | |
| Saline | 1 mL/kg | 0 ± 11.4 (28) | 0 ± 16.3 (27) | 0 ± 17.5 (27) |
| AN1284 | 0.05 | 10.8 ± 21.0 (10) ^b | 22.3 ± 18.4 (11) ^{*a} | 8.9 ± 21.9 (11) ^c |
| | 0.5 | 31.4 ± 15.6 (15) ^{**} | 37.5 ± 17.4 (13) ^{**} | 35.6 ± 16.1 (15) ^{**} |
| | 2.5 | 25.0 ± 26.0 (15) ^{**} | 7.9 ± 14.3 (11) ^b | 31.4 ± 15.8 (10) ^{**} |
| Vehicle | 1 mL/kg | 0 ± 15.7 (12) | 0 ± 6.1 (6) | 0 ± 18.4 (8) |
| AN1422 | 0.44 | 11.4 ± 18.6 (11) ^d | 9.53 ± 21.9 (9) | 20.5 ± 16.8 (9) |
| | 2.2 | 26.2 ± 17.8 (15) ^{**} | 17.7 ± 18.1 (8) | 20.1 ± 18.1 (8) |
| <i>Oral</i> | | | | |
| Saline | 1 mL/kg | 0 ± 12.4 (12) | 0 ± 18.4 (16) | 0 ± 15.5 (15) |
| AN1284 | 0.5 | 17.6 ± 20.9 (11) [*] | 19.9 ± 17.2 (8) ^{*e} | 34.6 ± 17.3 (11) ^{**} |
| | 2.5 | 37.6 ± 19.0 (13) ^{**} | 36.2 ± 19.9 (16) ^{**} | 28.1 ± 14.3 (12) ^{**} |
| | 10 | 15.7 ± 16.9 (11) [*] | 19.3 ± 17.3 (13) ^{*e} | 3.9 ± 18.1 (11) ^g |

Data represent mean % reduction in IL-6 in mice injected with LPS 5 mg/kg ip, induced by drug treatment compared to value in saline or vehicle pretreated controls \pm STD. () number of mice.

ANOVA: AN1284 **sc**. Plasma, F)3,64(= 11.80, $p=0.0001$; Brain, F)3,58(= 13.33, $p<0.0001$; Liver, F)3,59(= 15.41, $p=0.0001$.

ANOVA: AN1422 **sc**. Plasma, F)2,35(=7.08 $p=0.003$; Brain, F)2,20(=1.51, $p=0.245$; Liver, F (2,19) =2.21, $p=0.05$.

ANOVA: AN1284 **oral**. Plasma, F (3,42) = 7.86, $p=0.0001$; Brain, F (3,49) = 9.54, $p=0.0001$; Liver, F (3,32) = 9.07, $p=0.0001$. Significantly different from saline or vehicle, * $p<0.05$; ** $p<0.01$; significantly different from AN1284 (0.5 mg/kg) sc, ^a $p<0.05$, ^b $p<0.01$; significantly different from both AN1284 (0.5 mg/kg) and (2.5 mg/kg) sc, ^c $p<0.01$. Significantly different from AN1422 (2.2 mg/kg) sc, ^d $p<0.05$. Significantly different from AN1284 (2.5 mg/kg) gavage, ^e $p<0.05$; ^f $p<0.01$; significantly different from AN1284 (0.5 mg/kg) and (2.5 mg/kg) gavage, ^g $p<0.01$. Table 1 sc. Supplemental data [S5]

Table 1 oral Supplemental data [S6]

Table 2. Peak concentrations of AN1284 in plasma and tissues after subcutaneous and oral administration of 0.5 mg/kg and 2.5 mg/kg respectively.

| Tissue | Subcutaneous injection | | | Oral administration | | |
|---------------|--|---------------------|---------------------|--|---------------------|---------------------|
| | Peak conc. ^a (ng/gm or mL) | Tissue/ plasma | AN1422 ^b | Peak conc. ^a (ng/gm or mL) | Tissue/ plasma | AN1422 ^b |
| Plasma | 184 \pm 80 | | 44.4 | 32.8 \pm 14.9 | | 57.6 |
| Brain | 1070 \pm 319 | 5.8 (5.2-7.1) | 32.3 | 65.2 \pm 21.0 | 2.0 (1.8-2.3) | 96.8 |
| Liver | 285 \pm 140 | 1.6 (1.5-1.8) | 40.5 | 1553 \pm 519 | 47.3 (43.4-57.8) | 37.0 |
| Kidney | 3733 \pm 1182 | 20.3 (18.6-24.5) | 41.3 | 180 \pm 71 | 5.5 (5.3-6.1) | 65.8 |

^a Values represent the mean \pm STD of 6-11 replicates per tissue or plasma

^b Ratio of peak concentration of indole metabolite (AN1422) to that of AN1284

Table 2 sc Supplemental data [S3] Table 2 oral Supplemental data [S4]

Table 3. Concentrations in the liver of AN1284 and its indole metabolite (AN1422) after chronic administration of AN1284 to mice by sc implanted mini-pumps or in the drinking fluid

| Dose | Route | A. Conc AN1284 | B. Conc AN1422 | Ratio A/B |
|----------------|----------------|----------------|----------------|-----------|
| 0.5 mg/kg | sc | 285 | 114 | 2.7 |
| 2.5 mg/kg | oral | 1553 | 523 | 2.8 |
| 1 mg/kg/day | sc (mps) | 26.4 ± 3.1 | 7.8 ± 3.4 | 4.5 |
| 2.5 mg/kg/day | sc (mps) | 36.3 ± 6.7 | 13.6 ± 3.2 | 2.7 |
| 0.25 mg/kg/day | Drinking water | 15.3 ± 5.6 | 4.2 ± 3.4 | 5.0 |
| 0.5 mg/kg/day | Drinking water | 26.3 ± 11.7 | 7.5 ± 4.8 | 4.7 |
| 1 mg/kg/day | Drinking water | 36.4 ± 12.0 | 11.8 ± 6.7 | 3.8 |

Mini-pumps (mps)

Table 3 Supplemental data [S7]

Table 4. Urinary excretion of AN1284 and its metabolites after subcutaneous and oral administration

| Route | Average weight (g) | Dose of AN1284 (µg base/mouse) | Concentration in urine (ng/24h) | | | Ratio peak areas |
|----------|--------------------|--------------------------------|---------------------------------|-------------|-----------|--------------------|
| | | | AN1284 | AN1422 | AN1280 | Glucuronide/AN1280 |
| Sc (7) | 28.6 ± 2.3 | 12.6 ± 1.0 | 47.4 ± 27.2 | 31.4 ± 23.3 | 320 ± 177 | 2.2 ± 1.9 |
| Oral (7) | 29.7 ± 2.5 | 63.8 ± 1.7 | 4.7 ± 0.6 | 62.7 ± 14.8 | 774 ± 443 | 8.5 ± 7.6 |

Data represent mean ± STD or 24 h urine collections. (Number of mice). AN1422 is the indole and AN1280, the 7-OH derivative of AN1284. Table 4 Supplemental data [S8].

Figures

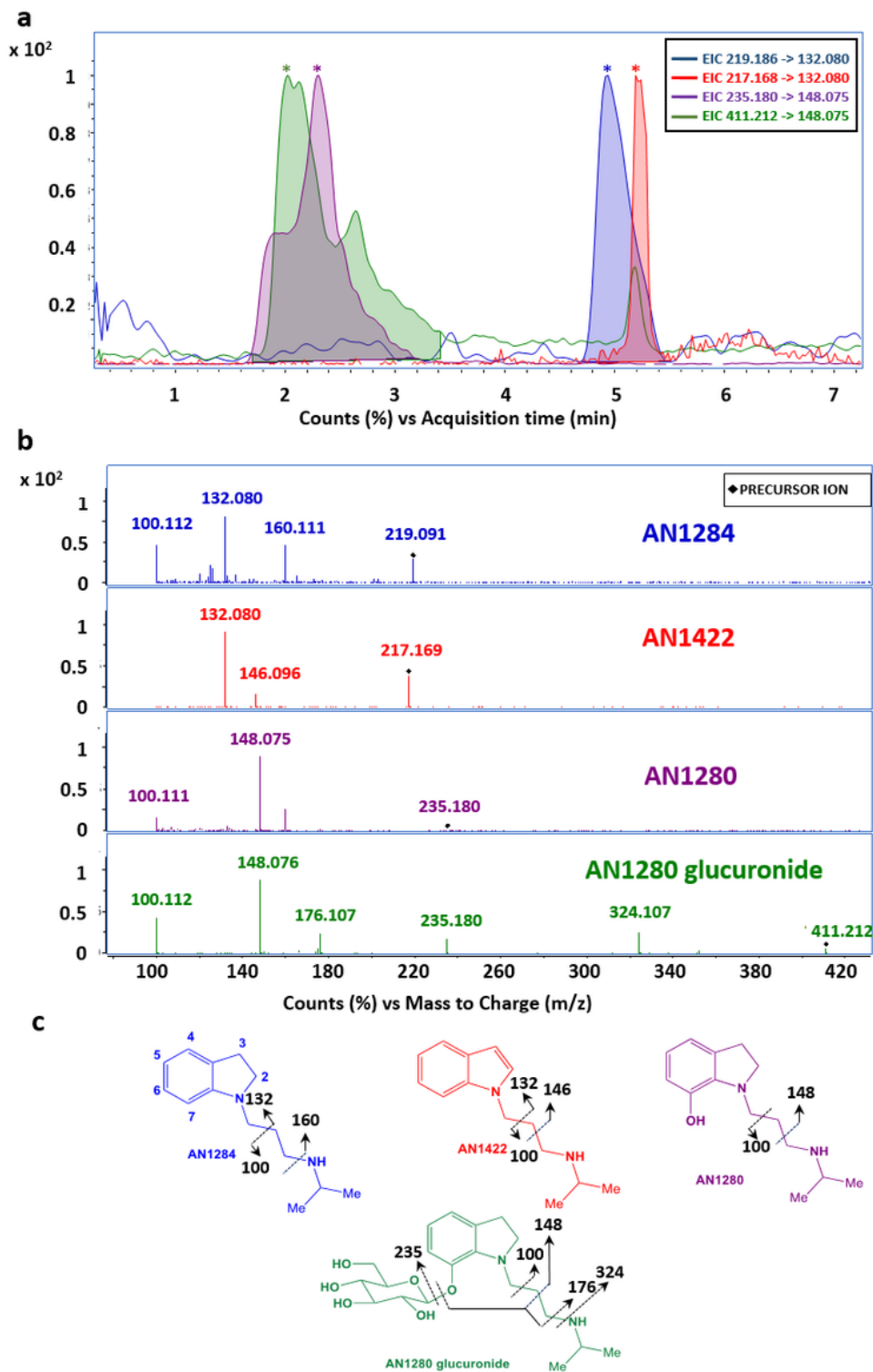


Figure 1

a) Extracted ion chromatogram of the protonated precursor ions [MH⁺]: AN1284 and its metabolites to their corresponding products ions. EIC = Extracted ion chromatogram. AN1422, hydroxy-AN1284 (AN1280) and AN1280-glucuronide (219.186 m/z, 217.170 m/z, 235.180 m/z and 411.212 m/z). The x-axis represents retention time (min), and the y-axis represents signal intensity. b) High resolution fragmentation mass spectra by collision-induced dissociation (MS/MS) of AN1284 and metabolites.

Precursor ions are indicated by ♦ in respective colors. c) Chemical structures of AN1284 and its metabolites. Fragmentation sites are shown by broken arrows.

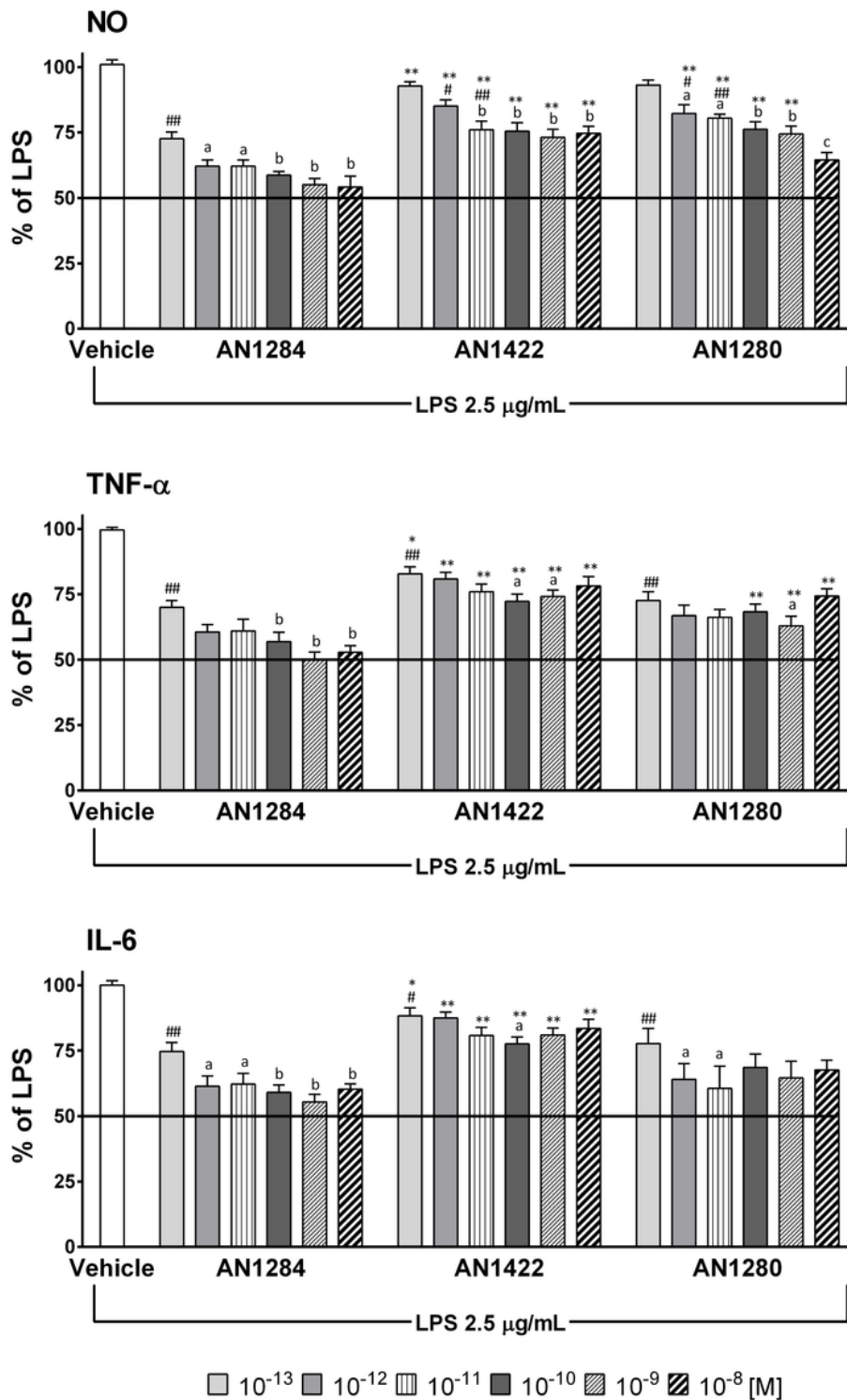
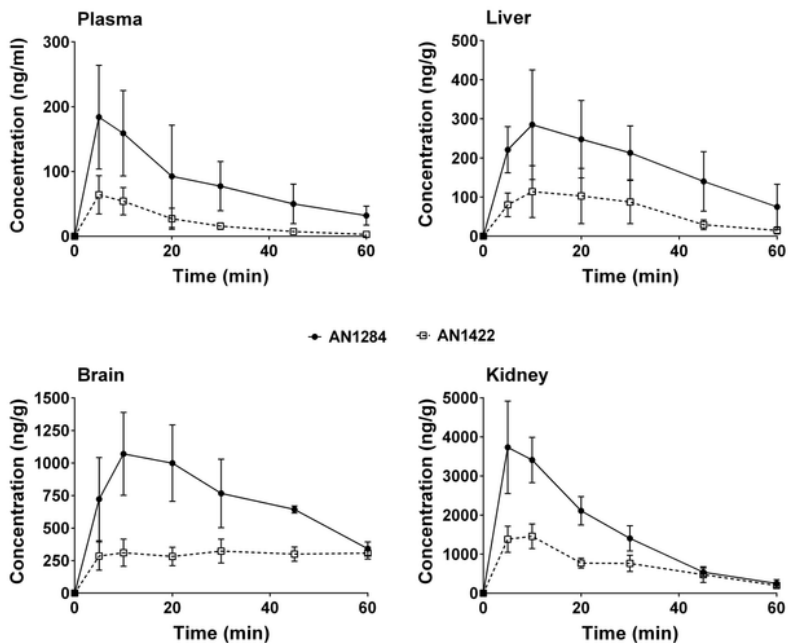


Figure 2

Reduction in release of NO, TNF-α and IL-6 by AN1284 and its metabolites from LPS activated RAW 264.7 macrophages. Data represent mean ± SEM from 12-24 replicates of each concentration of drug. ANOVA for vehicle and 7 concentrations of AN1284, 1422 and 1280 was F18,361 = 32.25, p < 0.0001 for NO,

F18,355 = 29.42, $p < 0.0001$ for TNF- α and F 18,342 = 16.25, $p < 0.0001$ for IL-6. Significantly different from vehicle, # $p < 0.05$, ## $p < 0.01$, significantly different from 0.1pM, a $p < 0.05$, b $p < 0.01$, c, significantly different from 1nM, significantly different from the same concentration of AN1284 * $p < 0.05$, ** $p < 0.01$. Supplemental data [S2].

Subcutaneous administration



Oral administration

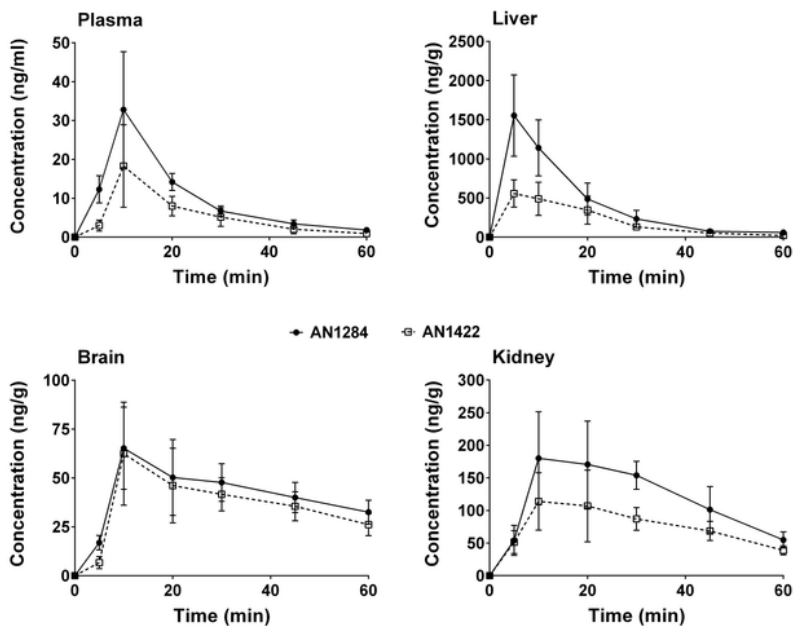


Figure 3

Concentration-time curves of AN1284 and AN1422 in plasma and tissues. a) After sc injection. b) After gavage. Data represent the mean \pm STD from 7-16 mice per time point. Fig. 3a Supplemental data [S3]. Fig. 3b Supplemental data [S4].

Metabolic oxidations of AN1284

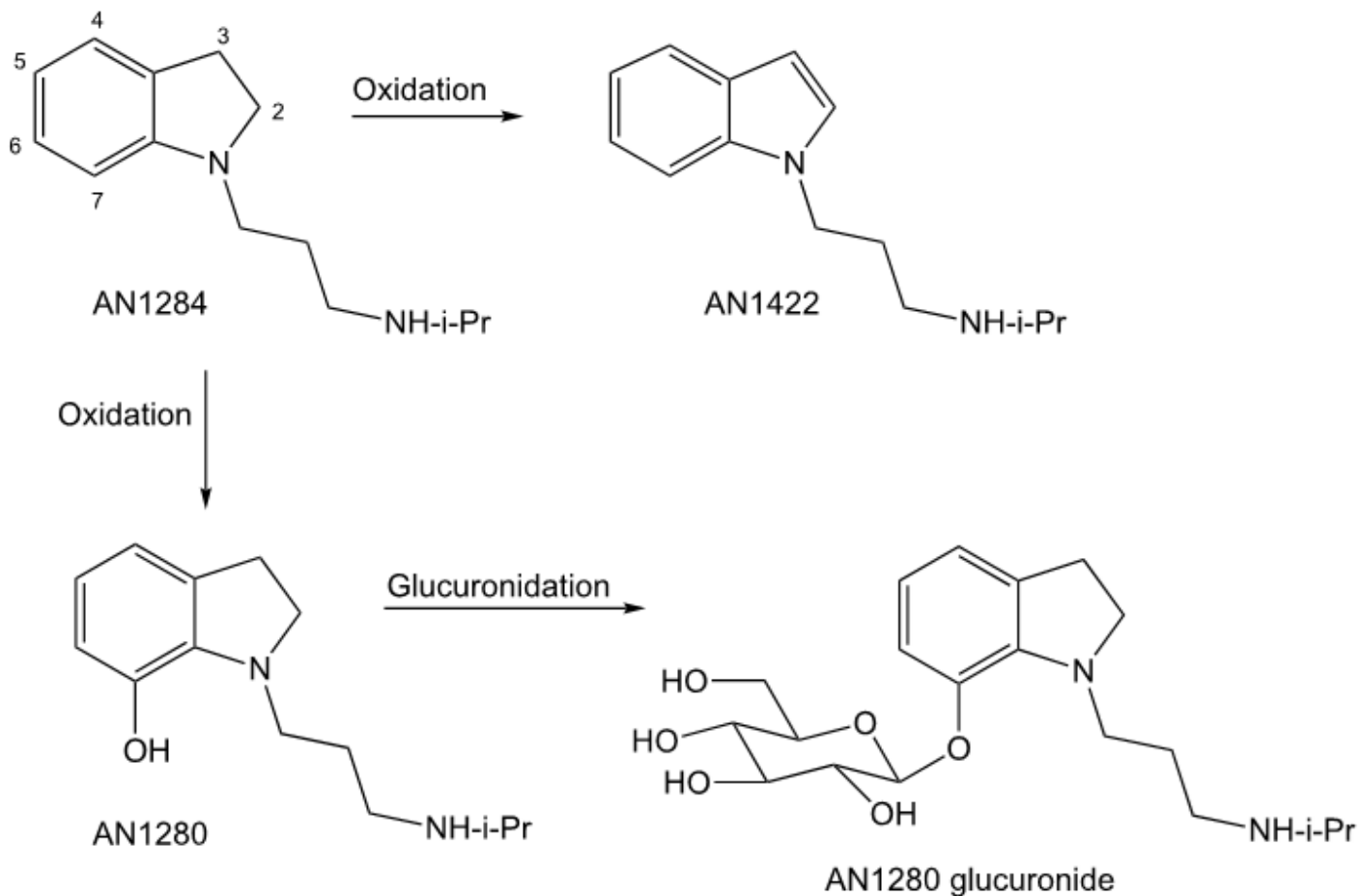


Figure 4

Metabolic oxidations and glucuronidation of AN1284.

Supplementary Files

This is a list of supplementary files associated with this preprint. Click to download.

- [S1.pdf](#)
- [S2.xlsx](#)
- [S3.xlsx](#)
- [S4.xlsx](#)
- [S5.xlsx](#)

- S6.xlsx
- S7.xlsx
- S8.xlsx